SSRG International Journal of Mechanical Engineering
ISSN: 2348 – 8360 /doi:10.14445/23488360/IJME-V8I11P103

Volume 8 Issue 11, 18-30, Nov, 2021

Cutting Tool Selection - Geometry, Workpiece, Tool Material: A Simulated, Library-Based Interactive Approach

Rahul Reddy Sandi[1], Chanikya Anasuri[2], Dr. Shyam Kumar. S[3]

[1]*Graduate, Department of Mechanical Engineering, Geethanjali College of Engineering and Technology, Telangana, India*
[2]*Graduate, Department of Mechanical Engineering, Geethanjali College of Engineering and Technology, Telangana, India*
[3]*Head of Department & Professor, Department of Mechanical Engineering, Geethanjali College of Engineering and Technology, Telangana, India*

Received Date: 15 October 2021
Revised Date: 20 November 2021
Accepted Date: 30 November 2021

Abstract *- In this paper, a single-point cutting tool-tip is subjected to various thermal and static loads at the tool interface with the workpiece. The machining of mild steel is analyzed for surface finish of the workpiece, metal removal rate, forces generated, deformation/ temperature generated, tool life using ANSYS so as to arrive at an appropriate cutting tool, and machining parameters. An algorithm has been developed to collect the data based on user-specified workpiece material and tool data from libraries. The parameters - feed rate and back rake angles are varied to suggest the best cutting tool/ signature using Python coding.*

Keywords - *Cutting tool, ANSYS, metal removal rate, deformation, algorithm*

I. INTRODUCTION

Cutting tool plays a vital role in the manufacturing industry. In this regard, the design and analysis of a single-point cutting tool is an important aspect of tool engineering. Various operating parameters of a cutting tool need a thorough study using existing theories. Management of the cutting process demands a good knowledge of the cutting tool's tribological characteristics as well as the arability of the workpiece. Development and application of new tool materials lead to the emergence of new generation materials resistant to vibrations, wear, high temperatures, thereby enabling machining without agents for cooling and lubrication.

From ancient times, Mild Steel has been widely used in various fabrication fields, viz. automotive, locomotive industries, and structural applications, due to its mechanical and recycling properties. In the fabrication process of mild steel applications, various cutting tools are employed in order to achieve the required output (surface finish, tolerances, etc.).

Cutting tool materials such as High-Speed Steel (HSS), Cubic Boron Nitride (CBN), Ceramics, Cemented carbides, Diamonds, Satellites, etc., have been used for machining operations. In this paper, HSS, Tungsten Cemented Carbide, and Silicon nitride (ceramic) have been considered as cutting tool materials.

For the development of this paper, various parameters like cutting forces, heat generated, temperature rise, tool life, etc., have been considered in combination with tool materials above said and these results have been analyzed and validated through simulation software.

II. LITERATURE REVIEW

A. Why is the study of cutting tools important? A **cutting tool** removes material from the work piece by means of shear deformation. Cutting may be achieved by a single-point or multipoint tool. The geometry of the cutting tool plays a vital role apart from the relative motion between the tool and workpiece imparted by the machine tool. The workpiece and cutting tool materials [1] have been considered with a database facility for an extension.

Surface finish, metal removal rate, tool life, the temperature generated, etc., largely depend on the cutting tool material and the workpiece material apart from the machining conditions.

B. Work Piece Material

a) Mild steel: Mild steel is a category of carbon steel with a low amount of carbon – it is also known as "low carbon steel." Based on the source, the range of carbon present in mild steel may vary between 0.05% and 0.25% by weight, in contrast to the high carbon steels with carbon content in the range of 0.30% - 2.0%. Mechanical properties of mild steel material are listed below from the available data and used for the analysis of the machining process.

Table I: Mild steel Mechanical properties

Mechanical Properties	Metric
Tensile strength, ultimate	440 MPa
Tensile strength, yield	370 MPa
Elongation at break (in 50 mm)	15.0 %
Reduction of area	40.0 %
Modulus of elasticity	205 GPa
Bulk modulus	140 GPa
Poisson's ratio	0.290
Machinability (based on AISI 1212 steel. As 100% machinability)	70 %
Shear modulus	80.0GPa

C. Cutting Tool Materials

In order to conduct a detailed study on working parameters and their effect, workpiece and tool material combination is restricted to the following tool materials. However, this approach may be extended for several other combinations, in similar lines using the algorithm/ program developed in the present work.

a) High-Speed Steel (HSS) is a premier cutting tool material and is a major subset of tool steels. Cutting tools are subjected to intense friction, heat, and extreme wear; and hence required to have high wear resistance, hardness, and red hardness. HSS cutting tools are formed from a blank of high-speed steel, followed by a cutting profile generated and hardened and tempered to HRC 62-68.

b) Tungsten Cemented Carbide (WC): **Cemented carbide** is a hard material that is extensively used as a cutting tool material. Tungsten carbide is formed by metallic bonding and used as a cutting tool material because of its ability to maintain a sharp **cutting** edge. WC tools produce a better finish on parts, and their temperature resistance allows faster machining.

c) Silicon Nitride (SiN) is a hard, brittle, heat-resistant, and corrosion-resistant material made by shaping and then firing a nonmetallic mineral, such as clay, at a high temperature. Silicon nitride has superior high-temperature capabilities to most other cutting tool materials. In addition, its low thermal expansion coefficient gives good thermal shock resistance when compared to most other ceramic materials.

Table II: Properties of cutting tool materials

No.	Properties	HSS	WC	SiN
1.	Young's Modulus	200 GPa	700 GPa	470 GPa
2.	Density	8138 Kg/m^3	15.63 g/cm^3	4 g/cm^3
3.	Melting Point	1430^0c	2803^0 c	>2000^0c
4.	Shear Strength	2500 MPa	2760 MPa	120 MPa
5.	Tensile Strength	760 MPa	344 MPa	1138 MPa
6.	Compressive Strength	3250 MPa	2700 MPa	2400 MPa
7.	Poisson's Ratio	0.29	0.31	0.20
8.	Thermal Conductivity	22 W/m-k	110 W/m-k	160 W/m-k
9.	Specific Heat Capacity	440 J/Kg-k	340 J/Kg-k	760 J/Kg-k
10.	Thermal Exp. Coefficient	10 µ/k	5.5µ/k	<10 µ/k

D. Geometry, Design, and Analysis of cutting tool

While machining, the cutting forces generated largely depend on the geometry of the cutting tool for a specified combination of tool and workpiece material. Hence, utmost attention is required on the geometry of the cutting tool.

a) Design & Geometry of tool:

Geometry iteration includes two parts, viz.

1. Geometrical modeling of the Tool.
2. Arriving at forces acting on the tool.

b) The geometry of Tool:

The tool signature, as shown in Figure 1, has the salient profile parameters [2], as below listed.

α_b – Back rake angle α_s – Side rake angle

θ_e – End relief angle

θ_s – Side relief angle

C_e – End cutting edge angle

C_s – Side cutting edge angle

1) Side Cutting Edge Angle: Viewed from above looking down on the cutting tool, it is the angle formed between the side flank of the tool and a line perpendicular to the workpiece centerline, also called principal cutting angle or lead angle. It may vary from 0 to 90°.

If the side cutting edge angle is low, forces coming onto the tool will decrease, and as a result, the power consumption will be minimal. Also, the surface finish improves with an increase in the side cutting edge angle and vice-versa.

2) End Cutting Edge Angle: The end cutting edge angle is the angle between the end cutting edge and a line perpendicular to the shank of the tool. End cutting edge angle ranges from 4° - 30°. End cutting edge angle prevents rubbing between the end of the tool and the workpiece. If the end cutting edge angle is low, it will cause vibration because of excessive tool contact with the work piece. Surface finish deuterates with an increase in end cutting edge angle and vice-versa.

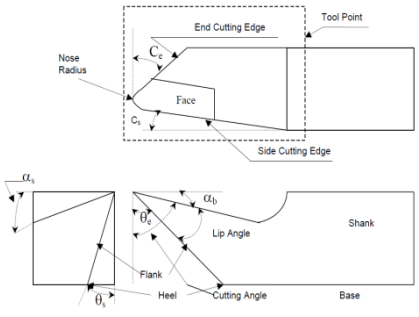

Fig 1. Single point cutting tool

3) Side Relief Angle: Viewed behind the tool down the length of the tool holder, it is the angle formed by the side flank of the tool and a vertical line down to the floor. It is the angle that prevents interference of the tool into the workpiece material. The relief angle generally ranges between 5° - 15°.

4) End Relief Angle: Viewed from the side facing the end of the workpiece, it is the angle formed by the end flank of the tool and a vertical line down to the floor. It is the angle that allows clearance between the tool to cut without rubbing on the workpiece. Relief angles generally range between 5° to 15°.

5) Back Rake Angle: Back rake angle is the angle between a face of the tool and a line parallel to the base of the tool, measured in a perpendicular plane through the side cutting edge. The back rake angle is in the range of 7° to 10° is preferable.

***6) Side Rake Angle*:** If viewed behind the tool down the length of the tool holder, it is the angle formed by the face of the tool and the centerline of the workpiece. The significance of the side rake angle is that it prevents rubbing action between tool and workpiece.

***7) Nose radius*:** It is provided to increase the strength of the tip of the tool and to improve the surface finish of the workpiece. The surface finish will be good if the radius is high. Higher nose radius results in increased tool-workpiece contact, thus increased friction, power consumption, and vibrations. Generally, the nose radius ranges from 1-3 mm.

Signature of a Single Point Cutting Tool:

All the tool angles are considered with reference to the cutting edge and are, therefore, normal to the cutting edge. The best way to specify tool angle is by the help of a standardized abbreviated system called tool signature or tool character. The signature of a single-point cutting tool is listed in the order of rake angles (back and side), relief angles (end and side), cutting edge angles (end and side), and nose radius.

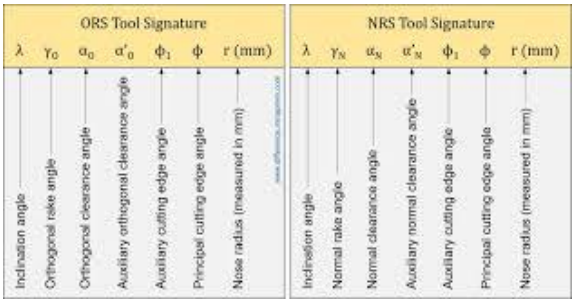

Fig 2. Tool Signature

E. Taylor's Tool Life Equation

Tool life indicates the period of satisfactory performance or service rendered by a new tool or a cutting point till its functional failure [3], [4] & [5].

With the slope, n and intercept, c, Taylor derived the simple equation

$VT^n = C$

where,

n, Taylor's tool life exponent

T, Tool life

The values of both 'n' and 'C' depend mainly on the tool and workpiece material and the cutting environment (cutting fluid application).

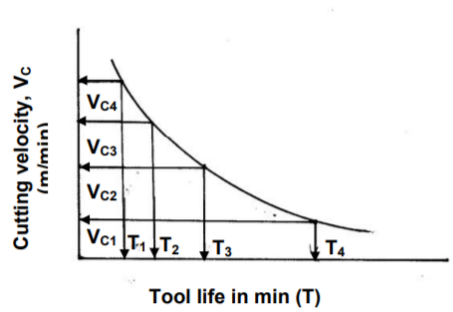

Fig 3. V vs. T Graph

Values of Taylor exponents(n) and constants(C) are taken from the below Table6 for different materials.

Table III: Taylor's exponent(n) and constant (C)

Tool Material	n	C (m/min)
HSS		
Non-steel work	0.125	120
Steel work	0.125	70
Tungsten Cemented Carbide (WC)		
Non-steel work	0.25	900
Steel work	0.25	500
Ceramic (SiN)		
Steel work	0.6	3000

III. DESIGN AND CALCULATIONS:

The force system on a cutting tool is broadly classified into two types [6]:

1. Forces are generated between the tool and the workpiece.
2. Force generated by the shearing of the chip and applied to the tool.

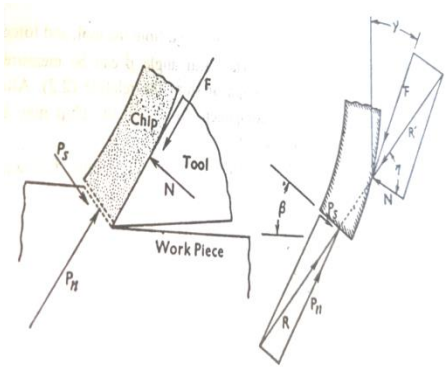

Fig 4. Forces & Angles

Cutting formulae have been chosen from the existing literature pertaining to orthogonal cutting. X, Y, Z cartesian system aligned to feed, depth of cut, and chip formation has been simplified with elimination of depth of cut.

P_x, the applied feed force

P_z, the generated cutting force

Formulae:

$$P_Z = K_C * d * f \quad (1)$$

Where,
f, feed rate, mm/rev, chosen from the past literature [7]
d, Depth of cut, mm, proposed a fixed value
K_C, specific cutting force N/mm^2, was chosen based on the feed values [8], Table 4.

Table IV. Specific Cutting Force

Workpiece Material	Tensile Strength (MPa)	Specific Cutting Force K_C (MPa)		
		0.1 mm/rev	0.2 mm/rev	0.3 mm/rev
Mild Steel	520	3610	3100	2720

The formulae used for calculations were inferred [9].

From equations 1, 2, and a chosen friction angle, P_X is obtained from the following relation.

$$\tan\eta = \frac{F}{N} = \frac{P_Z + P_Z \tan\gamma}{P_Z - P_x \tan\gamma} = \mu \quad (2)$$

The friction and related values for selected materials have been referred and adapted [10], [11], [12] & [13] in ensuing calculations.

Where,
η, frictional angle
μ, coefficient of friction
γ, rake angle
from relation 2, friction angle is obtained.

Table V: Frictional angles of selected materials

Material	μ	η
HSS	0.249	16.38
WC	0.621	31.84
SiN	0.7	34.99

Frictional angle value in Table 5 is obtained by using eqn. 2.

Merchant's Equation,

$$2\beta + \eta - \gamma = \frac{\pi}{2} \quad (3)$$

Where,
β, shear angle, value obtained from eqn. 3.

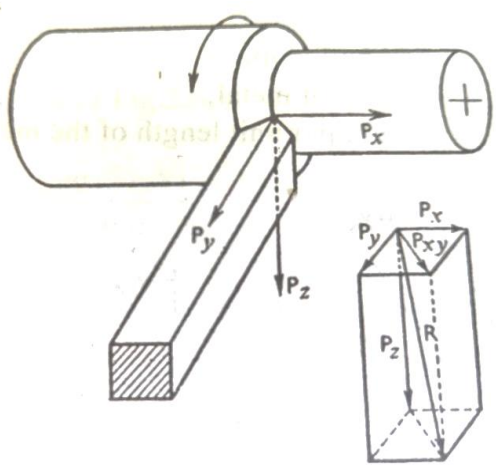

Fig 5. Forces on Cutting tool

From equation 3, shear angle **β** is obtained.

$$P_S = P_Z \cos\beta - P_X \sin\beta \quad (4)$$

$$P_N = P_X \cos\beta + P_Z \sin\beta \quad (5)$$

$$R = \sqrt{{P_S}^2 + {P_N}^2} \quad (6)$$

$$Work\ done(w) = R.V = P_Z * V \quad (7)$$

Where,

R = Resultant Force(N)

V = Cutting speed = $\frac{\pi DN}{1000}$ (m/min) (8)

Values of cutting speeds, V, are taken from table 6 to calculate spindle speed, N.

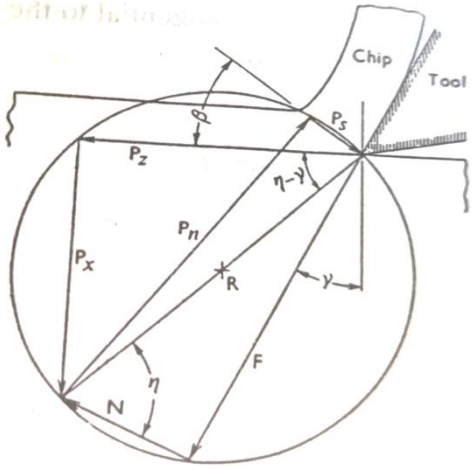

Fig 6. Merchant Circle

Table VI: Cutting speeds (m/min) of various materials

Material	Drilling	Turning	Shaping
Mild steel	25	30	20
Cast iron	15	15	10
Stainless steel	20	20	15
Bronze	55	60	30
Brass	50	60	30

D = Diameter of workpiece = 25mm

N = Spindle speed = 390rpm

Heat generated = Q_S = $^{W}/_{427}$ Kcal/min (9)

$$Q_S = R * V\ (W) \quad (10)$$

$$F_r = P_x cos\Upsilon + P_z sin\Upsilon \quad (11)$$

$$Q_R = {}^{(F_R * V)}/_{\lambda} \quad (12)$$

Where,

λ, chip thickness ratio (t_1/t_2), t_1 = 0.5, t_2 = 0.8

F_R, Frictional cutting force

$P_Z = F_C = Cutting\ force$

$$Q = Q_S + Q_R \quad (13)$$

Q, Total heat generated in watts

Q_S, Heat generated between tool and workpiece interface in watts

Q_R, Heat generated between tool and chip interface due to friction in watts

$$Q = C\Delta T \quad (14)$$

C = specific heat of tool material

$$Q = C(T_i - T_f) \quad (15)$$

Metal Removal Rate, MRR = $d * f * V$ (16)

Surface roughness = $f^2/8 * R\_n$ (17)

Where,

R_n, Nose radius in mm

Power requirement, P = $R * V$ (18)

Machining Time, T_N = $L/f * N$ (19)

Where,

Length of tool travel, L in mm

A Python code (not appended here) is developed to reduce monotonous design efforts and related calculations.

The following cutting tool geometry has been chosen for the present study from the past literature.

Dimensions of Cutting Tool:

Shank - 68 x 14 x 12 mm

Back rake angle – (8^0-10^0)

Side rake angle – 7^0

End clearance/relief angle – 20^0

Side clearance/relief angle – 10^0

End cutting edge angle – 15^0

Side cutting edge angle - 10^0

Nose radius – 1mm

IV. PYTHON CODE

To reduce monotonous calculations and to facilitate database enhancement, a Python code is developed with the following logic

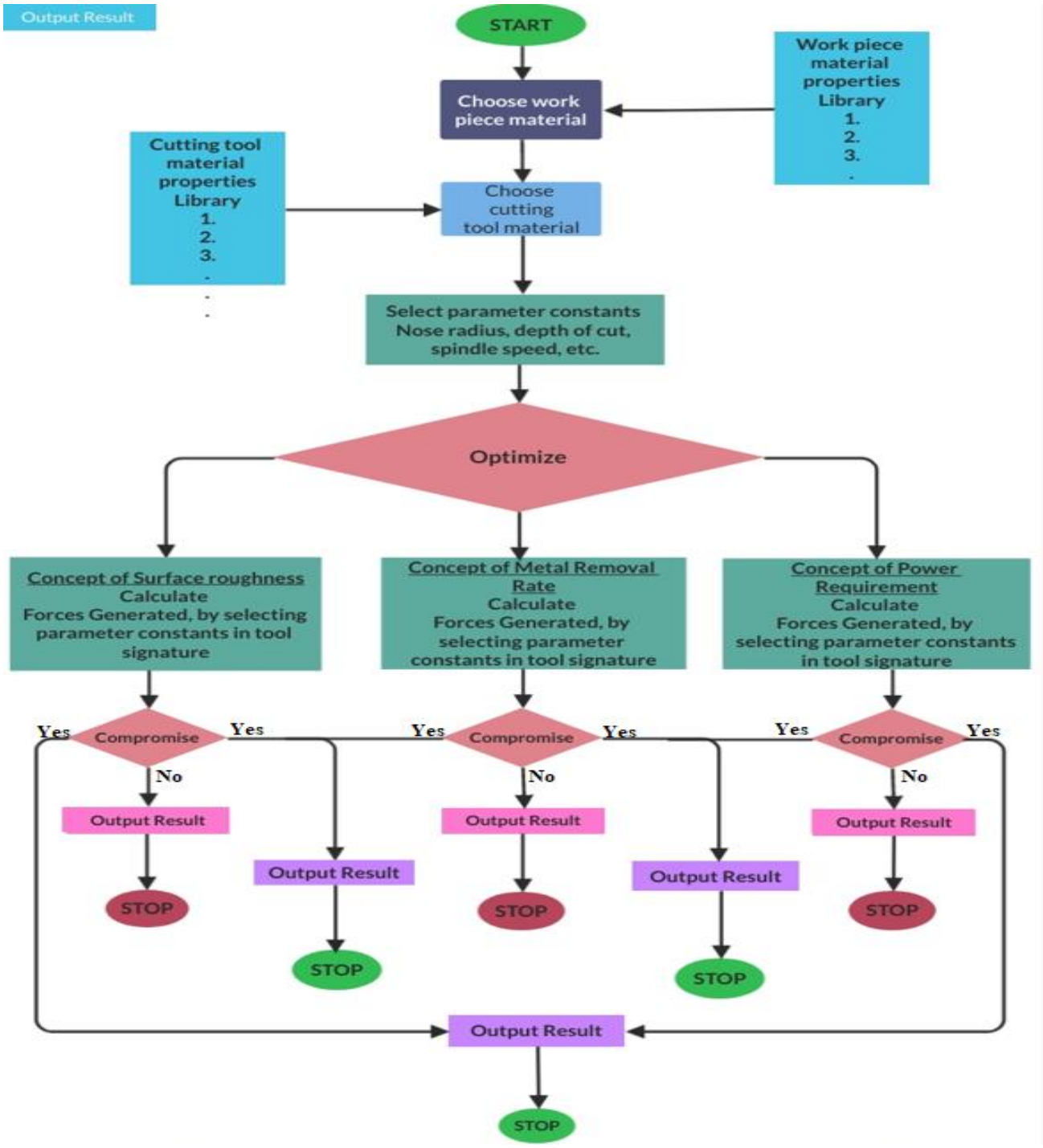

Fig 7. Algorithm 1: used to obtain best feed rate and rake angle

Fig 8. Algorithm 2: used to obtain best cutting tool material corresponding to best rake angle and best feed rate

V. RESULTS

For various combinations of Cutting tool material and machining conditions, metal removal rate, temperature-induced, and surface roughness are predicted through the Python coding and are presented below. The generated data is used for the optimization of tool signature and selection of tool material based on the user interest.

Table VII: HSS Results

Rake angle	Feed	K_C	β	PZ	PX	PS	PN	F	N	QS	QR	Q	TF
8	0.1	3610	40.8	180.5	-3698.07	2503.9	-2694.8	205.86	700.2	1851.2	80.41	1931.61	29.19
	0.2	3100	40.8	310	-6351.2	4360.5	-4628.1	353.56	1202.6	3179.3	138.109	3317.409	32.21
	0.3	2720	40.8	408	-8359.07	5739	-6091.3	465.34	1582.79	4184.51	181.773	4366.283	34.49
9	0.1	3610	41.31	180.5	-3350.6	2346.7	2393.82	209.08	711.18	1677.72	81.67	1759.39	28.82
	0.2	3100	41.31	310	-5754.5	4030.47	-4111.2	359.09	1221.42	2881.42	140.26	3021.68	31.56
	0.3	2720	41.31	408	-7573.16	5304.2	5410.59	472.62	1607.47	3792.07	184.617	3976.687	33.64
10	0.1	3610	42.81	180.5	-3072.13	2161.17	2154.24	212.32	722.19	1538.71	82.93	1621.64	28.52
	0.2	3100	42.81	310	-5276.4	3711.8	-3699.9	364.66	1240.37	2642.74	142.44	2785.18	31.05
	0.3	2720	42.81	408	-6944.2	4885	4869.42	479.94	1632.4	3478.08	187.47	3665.55	32.96

Table VIII: Tungsten Cemented Carbide Results

Rake angle	Feed	K_C	β	PZ	PX	PS	PN	F	N	QS	QR	Q	TF
8	0.1	3610	41.982	150.5	-4573.87	3152.32	-3265.58	205.86	823.31	288.71	83.68	372.39	27
	0.2	3100	41.982	320	-7855.4	5413.96	-5608.39	353.86	1414	3928.73	143.72	4072.45	47.13
	0.3	2720	41.982	408	-10338.7	7125	-7380.84	465.34	1861	3170.1	189.16	3359.26	54.12
9	0.1	3610	42.48	180.5	-4140.67	2929.45	-2931.9	209.08	863.31	2072.3	84.99	2157.29	36.72
	0.2	3100	42.48	320	-7111.4	5031.19	-5035.39	359.09	1436.3	3556.84	145.93	3702.77	45.72
	0.3	2720	42.48	408	-6513.1	4699.41	-4527.96	472.62	1439.5	3257.8	192.12	3449.92	43.74
10	0.1	3610	42.98	180.5	-3792.3	2717.42	-2651.36	212.32	849.18	1898.29	86.3	1984.59	35.78
	0.2	3100	42.98	320	-9359.52	6607.58	-6636	364.66	1960.3	4680.63	148.23	4828.86	51.24
	0.3	2720	42.98	408	-8572	6142.03	-5993.05	479.94	1919.47	4286.93	193.09	4480.02	49.35

Table IX: Ceramic (SiN) Results

Rake angle	Feed	K_C	β	PZ	PX	PS	PN	F	N	QS	QR	Q	TF
8	0.1	3610	31.505	180.5	-749.2	568.92	-582.92	205.56	292.11	407.22	60.45	467.67	25.53
	0.2	3100	31.505	310	-1364	977.09	-1000	353.56	372.19	699.39	103.98	803.37	25.91
	0.3	2720	31.505	408	-1795.2	1285.98	-1317.98	465.34	432.79	920.48	136.86	1057.34	26.201
9	0.1	3610	32.005	180.5	-745.46	548.15	-536.4	209.08	298.56	383.5	61.49	444.99	25.503
	0.2	3100	32.005	310	-1280.3	941.43	-921.43	359.09	383.27	658.64	105.61	764.25	25.86
	0.3	2720	32.005	408	-1685.04	-1239.04	-1212	472.62	447.38	806.86	139.005	945.865	26.14
10	0.1	3610	32.505	180.5	-694.92	525.65	-489	212.32	303.03	358.98	62.44	421.42	25.47
	0.2	3100	32.505	310	-1193.5	902.7	-839.9	364.66	390.99	616.55	107.25	723.8	25.82
	0.3	2720	32.505	408	-1570.8	1188.9	1105.19	479.99	457.9	811.46	141.18	952.64	26.08

A. Detailed drawings/ drafting's of 3 different cutting tools:

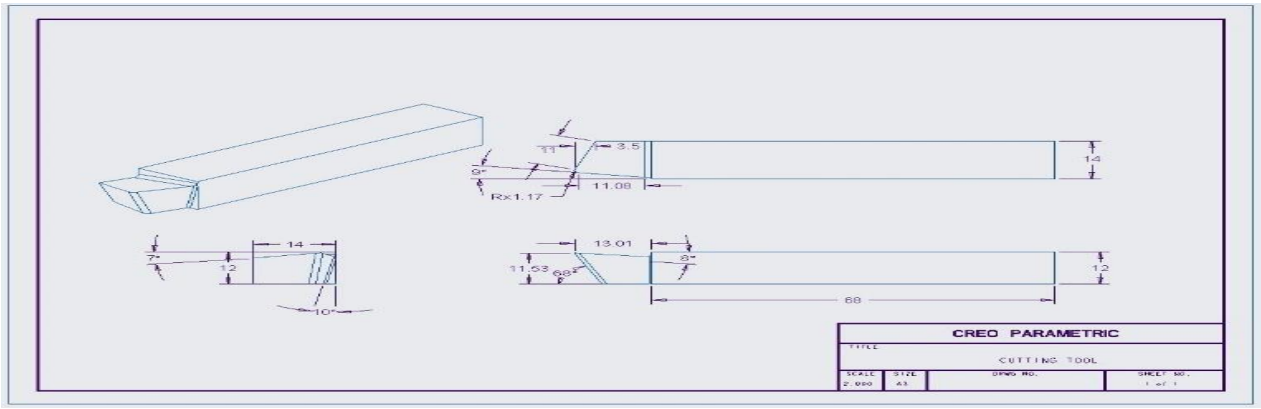

Fig 9. Cutting tool of back rake 8^0

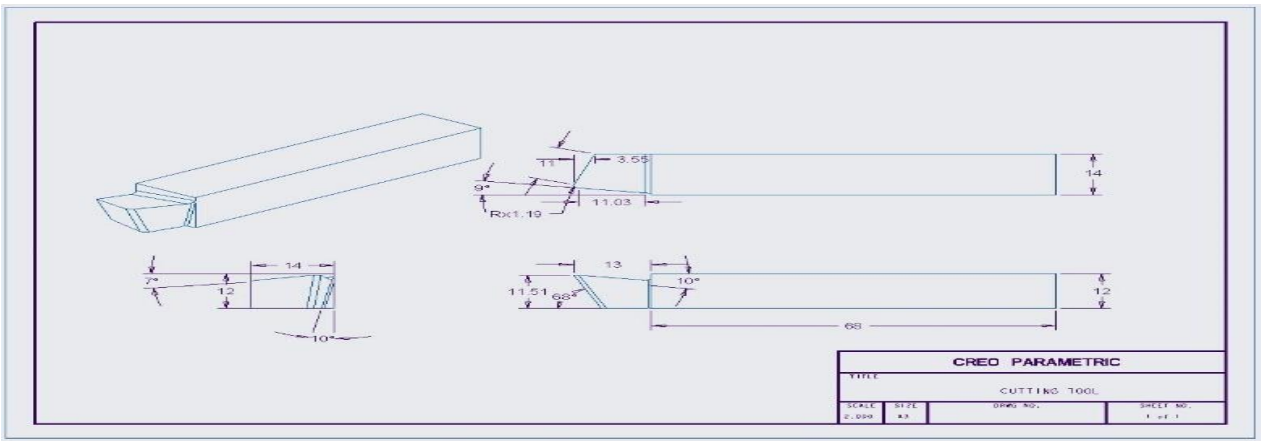

Fig 10. Cutting tool of back rake 9^0

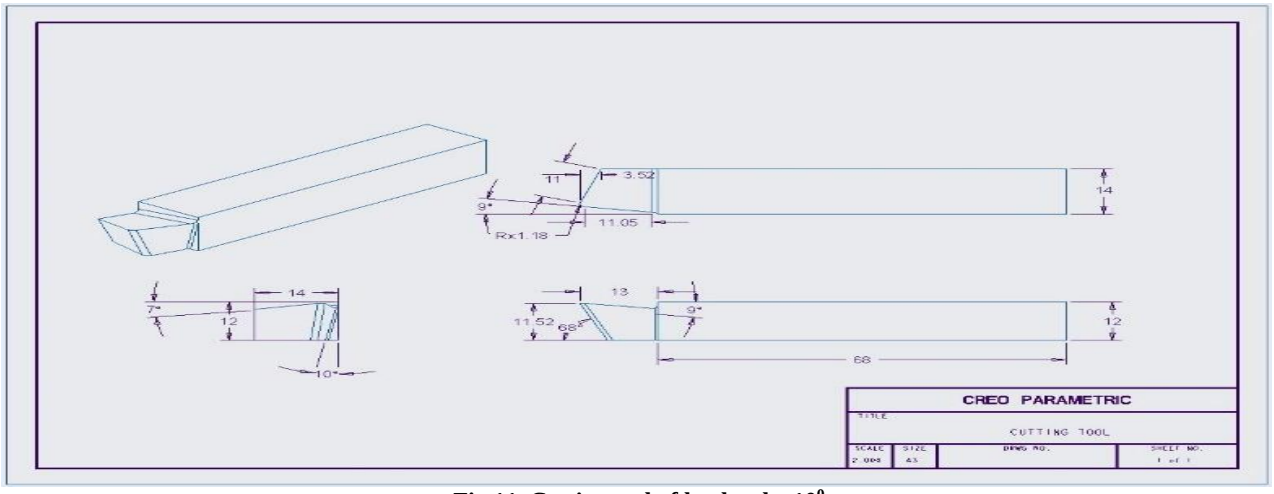

Fig 11. Cutting tool of back rake 10^0

VI. CUTTING TOOL SIMULATION USING ANSYS

Sample results obtained through ANSYS for the HSS tool with a rake angle of 8^0 at a feed rate of 0.1 mm/rev have been presented below, depicting tool behavior for equivalent stress, deformation, temperature, heat flux, and FoS.

Material: **High-Speed Steel (HSS)**
Rake Angle: **8^0**
Feed Rate: **0.1 mm/rev**

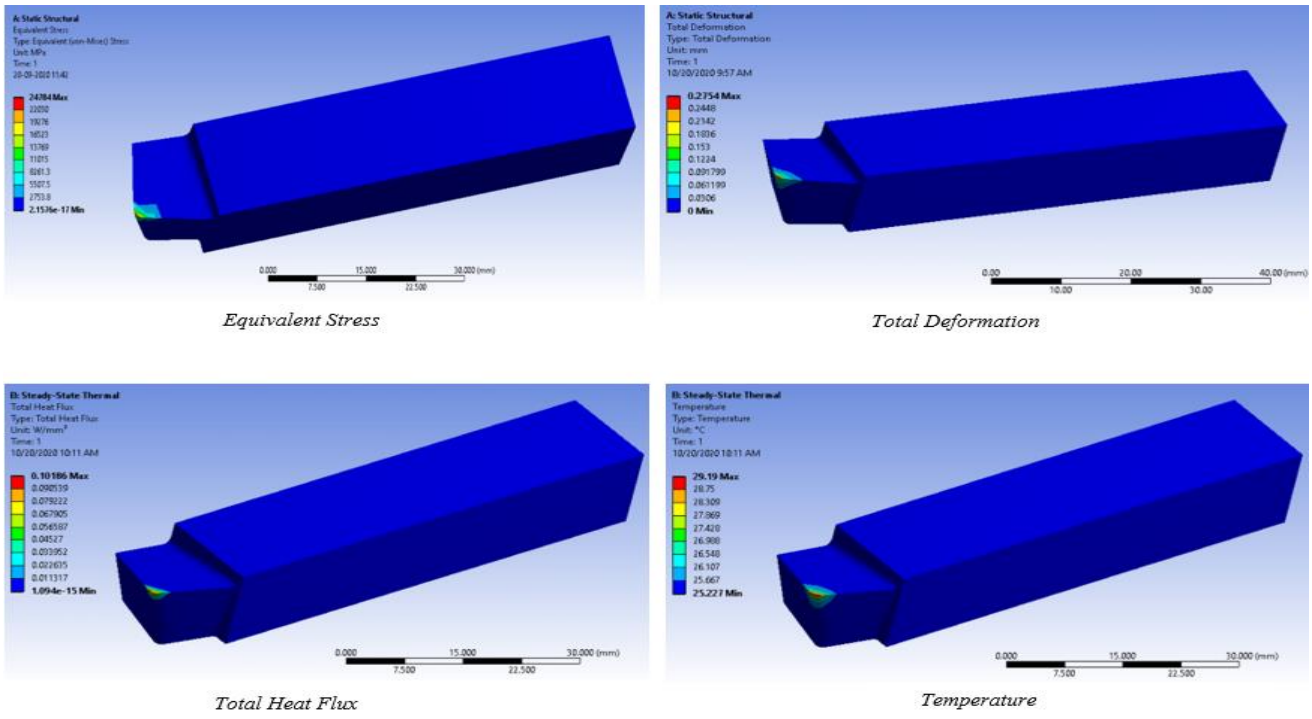

Fig 12. Analysis results from ANSYS

Single point cutting tool with 3 variant back rake angles, 3 different feeds and 5 output characteristics [14] & [15] (viz. Equivalent stress, deformation, temperature, heat flux and FoS) have been simulated using ANSYS for 3 different cutting tool materials.

Total 135 simulation results have been generated for optimization of Surface roughness, MRR, power requirement, forces generated and temperature induced through python coding.

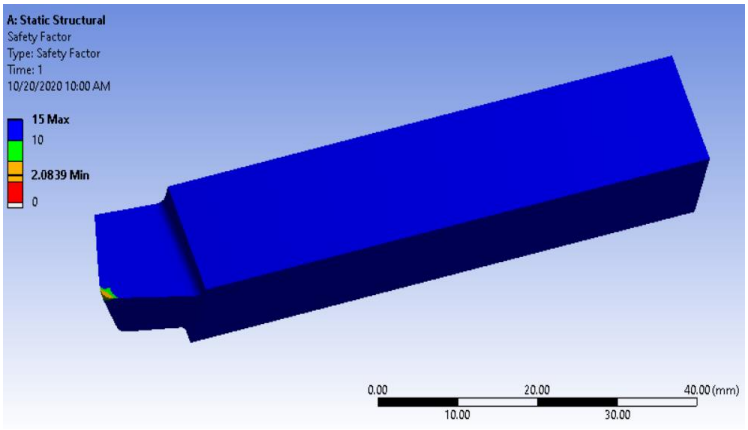

Fig 13. Factor of Safety from ANSYS

VII. RESULTS AND DISCUSSION

Table X: HSS Results

ϒ	λ	β	Feed	R	T	T_N	MRR	P	T_f	Q	Surface Roughness	Total Deformation	Equivalent stress	FoS
8^o	1.28	40.8	0.1	2678.5	769.813	2.564	4	91.75	29.1	1931.5	6.395	0.278	24784	2.033
			0.2	6358.7	769.813	1.282	8	157.5	32.2	3317	12.793	0.365	26218	1.639
			0.3	8368.9	769.813	0.854	12	201.4	34.4	4366.2	19.18	0.48	32619	1.245
9^o	1.28	41.3	0.1	3352.2	769.813	2.564	4	91.2	28.8	1759.3	6.395	0.191	9875.9	3.346
			0.2	5757.3	769.813	1.282	8	157.8	31.5	3021.6	12.793	0.328	16961	2.338
			0.3	7576.3	769.813	0.854	12	207.4	33.6	3976.6	19.18	0.433	22322	1.776
10^o	1.27	41.8	0.1	3051.4	769.813	2.564	4	91.75	29.5	1621.6	6.395	0.179	8944.6	3.697
			0.2	5290.8	769.813	1.282	8	157.3	31.05	2725.1	12.793	0.309	15362	2.582
			0.3	6898.4	769.813	0.854	12	207.4	32.9	3665.5	19.18	0.406	20223	1.962

Table XI: Tungsten Cemented Results

ϒ	λ	β	Feed	R	T	T_N	MRR	P	T_f	Q	Surface Roughness	Total Deformation	Equivalent Stress	FoS
8^o	1.23	81.9	0.1	4538.9	72223.854	2.564	4	91.75	27	112.3	6.395	0.095	17553	3.5072
			0.2	7795.1	72223.854	1.282	8	137.8	47.1	4071.7	12.793	0.163	30147	2.042
			0.3	10258.7	72223.854	0.854	12	207.4	54.12	5359.2	19.18	0.214	39674	1.551
9^o	1.22	43.4	0.1	4144.6	72223.854	2.564	4	91.73	36.7	2156.9	6.395	0.096	11810	4.573
			0.2	7118.6	72223.854	1.282	8	157.8	45.7	3703.8	12.793	0.132	18331	3.55
			0.3	6525.6	72223.854	0.854	12	207.4	43.7	3949.9	19.13	0.148	20284	2.954
10^o	1.3	42.9	0.1	3796.3	72223.854	2.564	4	91.75	35.7	1984.8	6.395	0.081	10769	4.462
			0.2	9364.2	72223.854	1.282	8	157.8	51.2	4828.9	12.793	0.183	24341	3.128
			0.3	8581.3	72223.854	0.854	12	307.4	49.3	4482.6	19.18	0.203	26283	2.467

Table XII: Ceramic (Silicon Nitride) Results

ϒ	λ	β	Feed	R	T	T_N	MRR	P	T_f	Q	Surface Roughness	Total Deformation	Equivalent Stress	FoS
8^o	1.71	31.5	0.1	814.5	2095.892	2.564	4	91.95	25.5	467.6	6.395	0.0129	3334	6.239
			0.2	1398.1	2095.892	1.282	8	157.8	25.9	803.32	12.793	0.0221	5724	3.654
			0.3	1841.4	2095.892	0.854	12	307.4	26.2	1037.3	19.18	0.0292	7536.7	2.76
9^o	1.78	32.05	0.1	766.9	2095.892	2.564	4	91.75	25.5	444.9	6.395	0.0125	3164.3	6.579

			0.2	1317.3	2095.892	1.282	8	157.8	25.8	784.2	12.793	0.0125	5142.7	3.634
			0.3	1733.2	2095.892	0.854	12	207.4	26.1	1006.3	19.18	0.0283	7151.9	2.911
10^o	1.71	32.5	0.1	717.9	2095.892	2.564	4	91.75	25.4	101.42	6.395	0.011	1863.3	11.529
			0.2	1233.3	2095.892	1.282	8	157.8	25.8	723.8	12.793	0.019	3201	6.712
			0.3	1322.7	2095.892	0.854	12	207.4	26.08	952.6	19.18	0.024	5090	4.232

Where:

ϒ- Rake Angle (^{o})
R – Resultant Force(N)
λ - Chip Thickness Ratio
T - Tool Life (min)
β - Shear Angle (^{o})
T_N - Machining Time (min)
P – Power (W)

MRR - Material Removal Rate (mm^3/rev)
Surface Roughness (μ m)
Equivalent Stress (MPa)
Total Deformation (mm)
FOS - Factor of Safety
T_F – Final temperature (^{0}c)
Q – Heat generated (W)

VIII. CONCLUSION

Observations reveal that at higher rake angles, the power consumption has been reduced for the same feed and MRR. Stresses produced in ceramic tools are much lower compared to the other two cutting materials. Mechanical stresses produced are favorable in HSS as compared to Tungsten cemented tools at lower rake angles.

The temperature produced in machining has been noticed as almost constant and very low as compared to the other two cutting tool materials (WC and HSS) with ceramic tools in the machining of Mild Steel. WC has a higher variation in cutting tool temperature with a change in feed rate.

Cutting tool deformations are high in HSS and low in Ceramics, whereas WC stands in between.

Hence a compromise is suggested between the output parameters with a user choice. Software code developed here is capable of suggesting cutting tool geometry and machining parameters based on the user's suggested power consumption, tooltip temperature, and surface roughness.

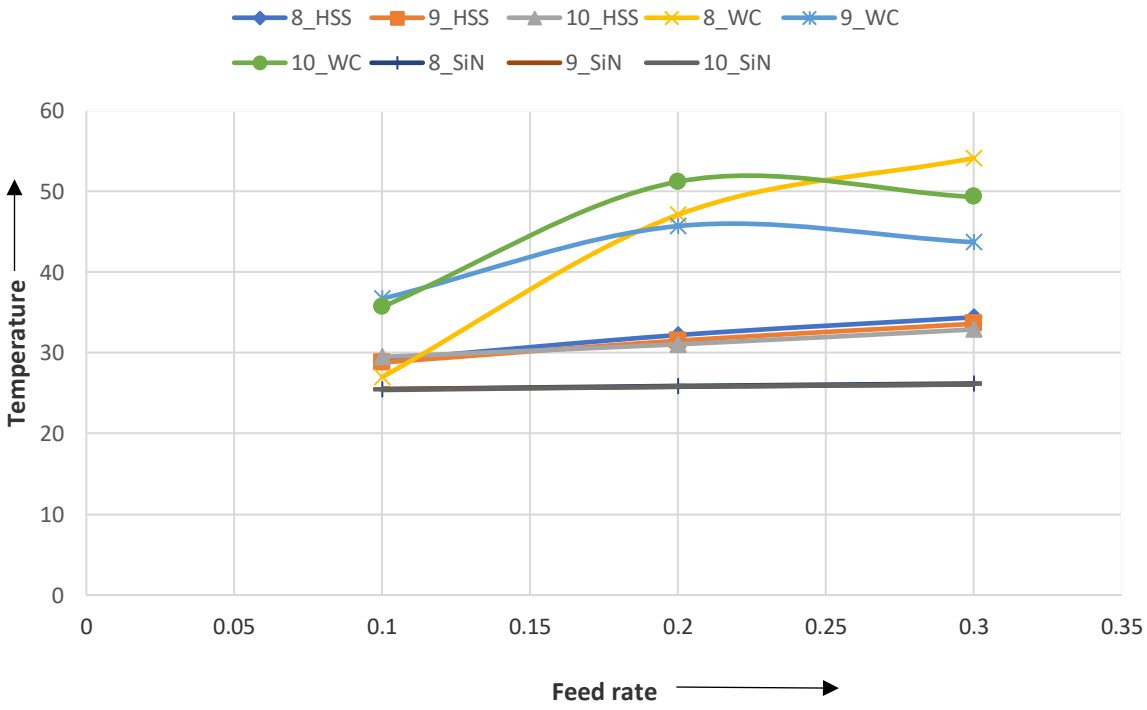

Graph I. Temperature vs. Feed Rate

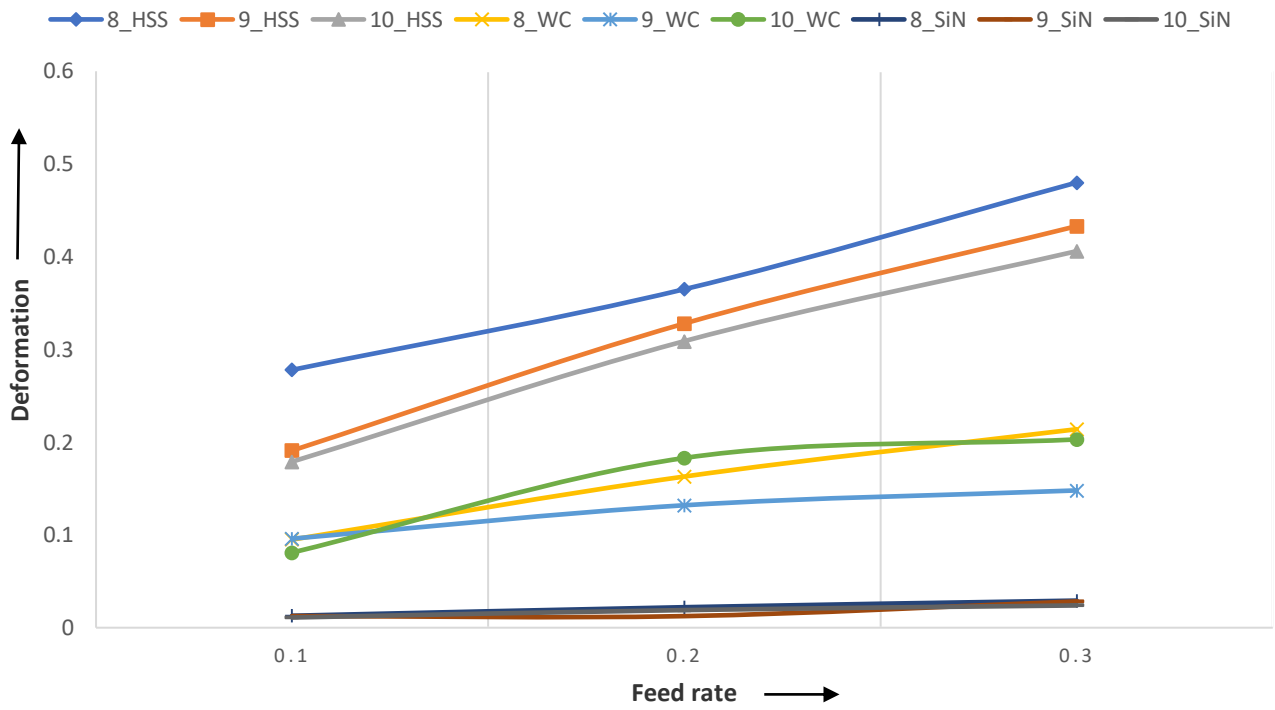

Graph II. Deformation vs. Feed Rate

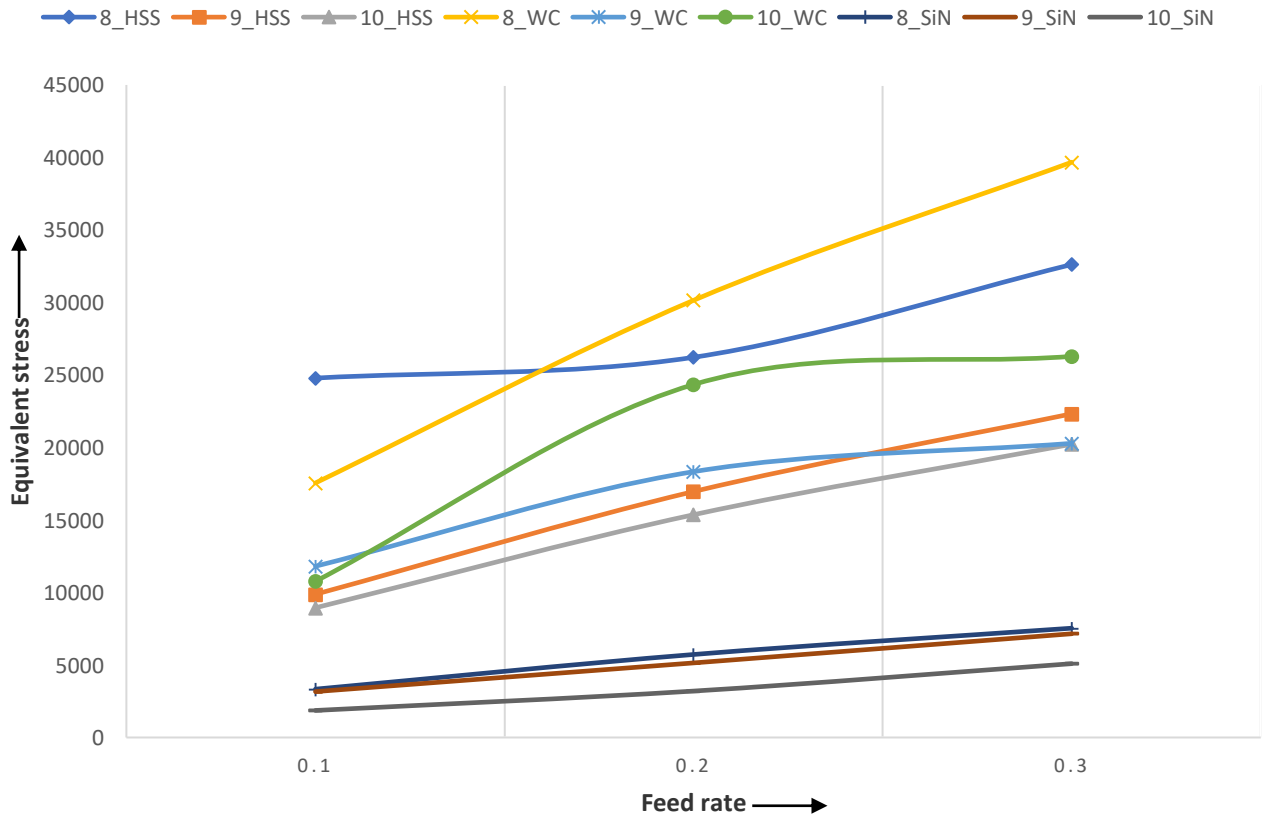

Graph III. Equivalent stress vs. Feed Rate

Final Results table:

Surface Roughness and Power requirement are optimized and compromised to obtain the best feed rate value. Forces generated are optimized to obtain the best rake angle for the corresponding best feed rate value.

Table XIII: Table obtained after Algorithm 1

Material	ϒ	λ	β	Feed	R	T	T_N	MRR	P	T_f	Q	Surface Roughness	Total Deformation	Equivalent Stress	FoS
HSS	9^o	1.28	41.3	0.1	3352.2	769.813	2.564	4	91.2	28.8	1759.3	6.395	0.191	9875.9	3.346
WC	9^o	1.22	43.4	0.1	4144.6	72223.854	2.564	4	91.73	36.7	2156.9	6.395	0.096	11810	4.573
SiN	10^o	1.71	32.5	0.1	717.9	2095.892	2.564	4	91.75	25.4	101.42	6.395	0.011	1863.3	11.529

In Algorithm 2, the Total Deformation value is limited to less than 0.1 mm, and the Final Temperature generated value is limited to less than 30 ^{0}C.

Table XIV: Final result obtained after Algorithm 2

Material	ϒ	λ	β	Feed	R	T	T_N	MRR	P	T_f	Q	Surface Roughness	Total Deformation	Equivalent Stress	FoS
SiN	10^o	1.71	32.5	0.1	717.9	2095.892	2.564	4	91.75	25.4	101.42	6.395	0.011	1863.3	11.529

IX. REFERENCES

[1] Materials Selection and Applications in Mechanical Engineering, book by A. Raman.

[2] Tool Geometry-related data of a single-point cutting tool. https://www.cobanengineering.com/Metal-Cutting-Technology/Terms-and-Definitions-of-the-Cutting-Tools-3.asp

[3] K. Kadirgama, K. A. Abou-El-Hossein, B. Mohammad, M. M. Noor, and S. M. Sapuan, Prediction of tool life by statistic method in end-milling operation, Scientific Research and Essay, 3 (5) (2008) 180-186.

[4] Cutting Tool Life in Production Technology, Prof. Naman M Dave.

[5] C.J.Rao[a], D.Sreeamulu[a], Arun TomMathew[b], Analysis of Tool Life during Turning Operation by Determining Optimal Process Parameters, Procedia Engineering, 97 (2014) 241-250.

[6] Workshop Technology (Volume – II) Machine Tools, by S. K. Hajra Choudhary, A. K. Hajra Choudhary, and Nirjhar Roy. Media Promoters & Publishers Pvt. Ltd., Mumbai(2007).

[7] Cutting speed, depth of cut, and feed-related information. https://openoregon.pressbooks.pub/manufacturingprocesses45/chapter/unit-2-speed-and-feed/

[8] Specific cutting force-related information. http://www.mitsubishicarbide.net/contents/mhg/enuk/html/product/technical_information/information/formula4.html

[9] Manufacturing Technology (Volume – II) Metal Cutting & Machine Tools, by P. N. Roy, Tata McGraw Hill Publications, New Delhi (2008).

[10] J. F. Archard, Wear Theory and Mechanisms, Wear Control Handbook, M. B. Peterson and W.O. Winer, eds., ASME, New York, NY, (1980) 35- 80.

[11] S. Dolinsek, J. Kopac, Mechanism and types of tool wear; particularities in advanced cutting materials, Journal of Achievements in Materials and Manufacturing Engineering, 19(1) 2006.

[12] K. C. Ludema, Friction, Wear, Lubrication a Textbook in Tribology, CRC Press, London, UK. (1996).

[13] D. Tabor, Friction and Wear – Developments over the last 50Years, Keynote Address, Proc. International Conf. Tribology –Friction, Lubrication, and Wear, 50 Years On, London, Inst. Mech. Eng., (1997) 157-72.

[14] W.S. Lin, The reliability analysis of cutting tools in the HSM processes, Archives of Materials Science and Engineering, 30(2) (2008) 97-100.

[15] Introduction to Finite Elements in Engineering, by Tirupati R. Chandrupatla and Ashok D. Belegundu, Prentice-Hall of India Pvt. Ltd. New Delhi(2002).